Preprints of the 19th World Congress
The International Federation of Automatic Control
Cape Town, South Africa. August 24-29, 2014

A Microgrid Library in a General Simulation Language

J. Salazar, F. Tadeo, C. de Prada

Department of System Engineering and Automatic Control
School of Industrial Engineering, University of Valladolid, 47011Valladolid, Spain
(e-mail: fernando@autom.uva.es)

Abstract: A library in the EcosimPro environment, developed with the objective of providing the tools needed to integrate MicroGrids into multi-domain simulations is presented. Thus, practical simulated components of renewable energy sources (photovoltaic arrays, wind turbines), diesel generators, power electronic interfaces (DC/AC or AC/DC/AC), energy storage devices (batteries) are developed, in order to integrate them with the existing libraries of loads (such as electrical systems, hydraulic systems, chemical engineering process, etc). Components in the library are designed so they can be parametrized from data sheet information by general engineers, and then graphically connected to simulate under variable conditions specific real-life Microgrids. With this, different configurations and control strategies for Microgrids can be tested when operating on the real process. After presenting the main ideas behind the dynamic modelling of the components, the application to a case study is presented.

Keywords: MicroGrid, Photovoltaic Arrays, Wind Turbine, Simulation Tools.

1. INTRODUCTION

The demand for Microgrids that provide electrical energy supply systems in isolated areas is increasing around the world, not only for supplying remote dwellings with electricity, but also for water pumping (Sallem et al., 2009), desalination (Gambier et al., 2011, Salazar et al. 2011b), and other uses. A MicroGrid (MG) is defined here as any set of power generation units, loads, storage and control systems, with the corresponding electrical connections that are locally connected. Photovoltaic panels are probably the most frequent locally generated renewable energy source, although sometimes they are combined with wind generators to partially compensate for variability of production, so these would be considered here. Also, to balance with the electricity production, batteries are also considered (to keep the Microgrid stability), together with backup diesel generators. One example of these Microgrids (extracted from Salazar et al., 2010a) is presented in Figure 1: The three-phase power supply system comprises photovoltaic panels, a wind turbine, a battery bank, and a Diesel Generator.

A central role in the operation of this kind of systems is provided by the control power electronics: The Solar Inverter changes the direct current electricity (DC) from a photovoltaic array into alternating current (AC), which is injected into the main AC bus of the system. The Wind Inverter converts the variable frequency voltage from wind generators into grid-conforming AC voltage. The Bidirectional Battery Inverter functions as an inverter or rectifier charger mode. In the inverter mode, it converts direct current (DC) from the battery bank into alternating current (AC) which is injected into the main AC bus of the system. In rectifier charger mode, the excess of power generated charges the battery bank (see, for example, Mohammedi et al., 2011).

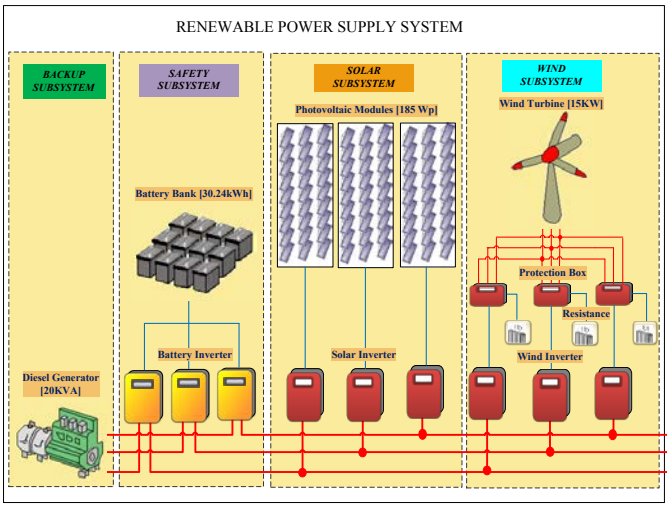

Fig. 1. Example of Microgrid with mixed Renewable Energy sources

Working with this kind of systems motivated us the creation of a library of simulated components that could be easily connected with existing models of typical loads (pumps, climatization systems, etc) in general simulations language. Of course there are very precise tools for simulating Microgrids (with loads that are frequently modelled as simple nonlinear systems using an equivalent circuit approach); the focus here is on providing to those engineers that are not specialized in Microgrid some tools to evaluate the effect of a Microgrid on each load.

For this, EcosimPro© was selected as simulation language, as it is a powerful modelling and simulation tool oriented towards multidomain simulations: the object oriented and non causal approach allows new simulations to be created using components from different libraries. In fact, components have already been developed and are extensively used in areas like Chemical Engineering (Garcia et al., 2002; Palacin et al., 2011), Life Support Systems (Pérez-Vara et al.,

2003; Ordónez et al., 2004), Nuclear Plants (Argüello-Tara et al., 2003), Space Support Systems (Moral et al., 2010), etc . Then our aim here is to add to the set of existing libraries a Microgrid library that can be connected to existing components to evaluate the effects of the Microgrid on the loads.

One advantage of EcosimPro (that is shared with other modern general simulation languages) is that it is possible to directly implement the mathematical equations that describe the system (this equations can be algebraic, differential, event-based, in difference, etc). Then the focus when developing components in these languages is in writing mathematical equations that describe the dynamics of the components at the time scale needed: once these equations are written, translating them into the simulation language is direct.

Thus, the paper presented here concentrates on presenting the models used for simulation of Microgrid components, which are selected to be precise enough in the time scale of minutes (given by the time dynamics of the loads), but quick enough so that the operation during many months can be evaluated in reasonable time using standard computing systems.

The paper is organized as follows: Section 2 presents some models used in the library for the MicroSources considered (PV arrays and wind turbines) which integrate the MicroGrid. Section 3 focuses on the modelling of the Microgrid controllers, considering the voltage and current inverter models. Finally, section 4 presents the application to a case study, showing how the developed tool can be integrated to effectively simulate real process.

2. MODELLING OF RENEWABLE ENERGY SOURCES FOR THE MICROGRID LIBRARY

As it has been mentioned before, modern general simulation languages makes possible to implement directly models written in terms of equations, so the focus of this section is to present the models selected for simulation of some of the most frequent energy sources in Microgrids (Photovoltaic Panels and Wind Turbines). The models are extracted from the literature, and are selected based on the precision in the time-scale proposed (minutes).

2.1 PV Array Models

2.1.1 Equivalent circuit model

Each solar cell that constitutes PV arrays is modelled as a p-n junction that converts solar radiation into DC current due to the photovoltaic effect. In order to have an adequate computational time, the equivalent circuit considered in the Microgrid library is a current source in parallel with a diode (see for example, Chouder et al., 2006).

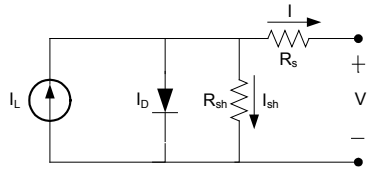

Fig. 2. Equivalent circuit used for modelling the solar cells

Under several assumptions (that the leakage current to the ground (*Ish*) is negligible, that the diode is conducting, that the produced current I_L is the one generated by the photovoltaic effect in open-loop I_{sc}, etc), the characteristic equation used for modelling the cell is:

$$I = I_{sc}\left[1 - exp\left(\frac{V + R_s I - V_{oc}}{V_t}\right)\right] \quad (2)$$

Thus, the mathematical model used to predict the power production of a whole PV array in the Microgrid library is:

$$I_{pv} = I_{scg}\left[1 - \exp\left(\frac{V_{pv} + R_{sg} I_{pv} - V_{ocg}}{V_t N_{sm} N_{sc}}\right)\right] \quad (3)$$

where V_{pv} is the output voltage of the PV array, I_{pv} is the output current of the PV array, R_{sg} is the series resistance of the PV array, I_{scg} is the short circuit current, V_{ocg} is the open circuit voltage, N_{sc} is the number of cells in series within the PV module, N_{sm} is the number of modules in series within the PV array and V_t is the thermal voltage.

2.1.2 Dependence with Temperature

If the temperature of the modules that contain the cells changes, the voltage and current outputs of the PV array change. This is modelled in the library by considering variations of the module open circuit voltage V_{ocm} and module short circuit current I_{scm} through experimental temperature coefficients β and α:

$$V_{ocm} = V_{ocm,stc}\left(1 + \frac{\beta(T_C - T_{ref})}{100}\right) \quad (4)$$

$$I_{scm} = \frac{I_{scm,stc} G}{1000}\left(1 + \frac{\alpha(T_C - T_{ref})}{100}\right) \quad (5)$$

where $I_{scm,stc}$ and $V_{ocm,stc}$ are short circuit current and open circuit voltage at Standard Test Conditions (STC), respectively.

To simulate the module operating temperature T_C (ºC) as a function of easily measurable variables, it is deduced from the environment temperature T_{env} (ºC) and the solar irradiation G (Wm^{-2}) is:

$$T_C = T_{env} + G\left(\frac{NOCT - 20}{800}\right) \quad (6)$$

where *NOCT* is the Nominal Operation Cell Temperature, (irradiance level of 1000 W/m², reference air mass of 1.5 solar spectral irradiance distribution and module junction temperature 25°C).

2.1.3 Maximum Power Tracking Algorithm

As it is well known, a Maximum Power Point Tracking (MPPT) technique makes possible to continuously deliver the highest possible power, even if irradiance and temperature vary. To optimize the nonlinear current-voltage characteristic varying with the irradiance and temperature several MPPT algorithms are used (see Trishan et al., 2007 for a review). In the first version of the library a basic MPPT model is used: the analytical derivative of the power with respect to voltage is used to estimate the Maximum Power Point. The equations can be then directly implemented and are the following:

$$V_{max} = (V_t N_{sm} N_{sc}) log\left(1 - \frac{I_{max}}{I_{scg}}\right) + V_{ocg} - I_{max} R_{sg} \quad (7)$$

$$\frac{dI}{dV} = \frac{-\frac{I_{scg}}{V_t N_{sm} N_{sc}} \exp\left(\frac{V_{\max} + I_{\max} R_{sg} - V_{ocg}}{V_t N_{sm} N_{sc}}\right)}{1 + \frac{I_{scg}}{V_t N_{sm} N_{sc}} \exp\left(\frac{V_{\max} + I_{\max} R_{sg} - V_{ocg}}{V_t N_{sm} N_{sc}}\right) R_{sg}} \quad (8)$$

$$I_{max} = -V_{\max} \frac{dI}{dV} \quad (9)$$

2.2 Wind Turbine

Wind turbines vary extensively in characteristics. The preliminary version of the library concentrates on variable speed wind turbines that follow the structure presented in Figure 3, which includes explicitly the possibility of modification of the blade pitch angle β_{ref} and the rated peak power T_{eref} by the Microgrid controllers. The models used for some of these components are now briefly discussed.

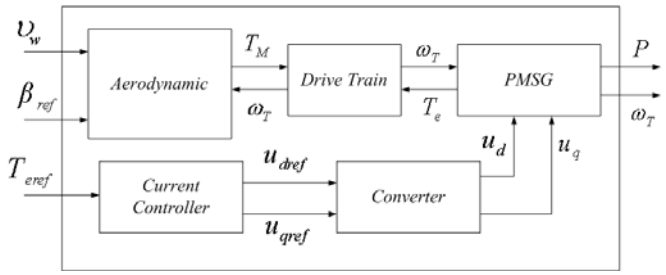

Fig. 3. Components of the Wind Turbine Model

2.2.1 Aerodynamics of the Wind Turbine Rotor

The fraction of the wind power extracted as mechanical power by the wind turbine is described by

$$P_M = \frac{1}{2} C_p(\beta,\lambda) \rho A \upsilon_w^3 \quad (11)$$

Where C_p is the power coefficient (discussed later), ρ is the air density, A is the area swept by the blades and υ_w is the wind speed.

The power coefficient is modeled as a function of the blade pitch angle β and the tip speed ratio λ following Raiambal at al. (2002) it is modelled in the library as

$$C_p(\lambda,\beta) = 0.71\left(\frac{230}{\sigma} - 0.4\beta - 20\right)\exp\left(\frac{-21}{\sigma}\right) + 0.00571\lambda, \quad (12)$$

where

$$\sigma = \left[\frac{1}{\lambda + 0.08\beta} - \frac{0.035}{\beta^3 + 1}\right]^{-1}, \quad (13)$$

and the tip speed ratio λ is the ratio between the blade tip speed and the wind speed υ_w:

$$\lambda = \frac{\omega_T R}{\upsilon_w} \quad (14)$$

ω_T being the turbine rotor speed and R the radius of the blades.

Variations in the blade angle decided by the Microgrid controller are not instantaneous, so the hydraulic actuator is modeled as a first order system:

$$\frac{\beta}{\beta_{ref}} = \frac{1}{\tau_{servo} s + 1} \quad (15)$$

2.2.2 Drive Train Model

The mechanical system of the wind turbine is modeled using a one-mass model (following, for example, Mei et al., 2005):

$$J_{total} \frac{d\omega_T}{dt} = T_M - T_e - F_r \omega_T \quad (16)$$

where $J_{total}=J_T+J_g$ is the moment of inertia of the whole drive train, with J_T and J_g being the moments of inertia of the turbine and the generator, respectively; F_r is the friction coefficient; T_e is the generator electromagnetic torque and the mechanical torque of the turbine T_M is given by

$$T_M = \frac{P_M}{\omega_T} = \frac{1}{2} \frac{C_p(\lambda,\beta)\rho A \upsilon_w^3}{\omega_T} \quad (17)$$

Detailed models of the current controller, converter and Permanent Magnet Synchronous Generator, can be found in Salazar et al. (2011a).

2.2.3 Local Controller

A summary of the local controller models (for details, see Salazar et al. 2011a) is now presented; the control strategy is assumed to depend on the operating regime in Figure 6:

- In Region I the turbine is modelled as running at the maximum efficiency to extract all power by adjusting the speed of the rotor;
- In Region III, the turbine is modelled as operating at the limit of generated power T_{eref} by varying the rotor speed ω_T and/or the reference of the pitch angle β_{ref};
- Region II is a transition region, with high but variable torque (see Rasila et al. 2003).
- Outside these regions the turbine is assumed to be stopped, not generating power.

3. MODELLING OF MICROGRID CONTROLLERS

This modelling based on two different operating conditions:

- Normal interconnected mode when the MicroGrid is connected to a small diesel engine in order to take/inject an amount of energy from/to it. Frequency and voltage references are provided by the diesel engine. All inverters present act like current sources (slaves), following the reference defined by the diesel engine.
- The isolated mode is assumed when the MicroGrid is not connected to a small diesel engine. Frequency and voltage references are provided by the inverter, which acts like a voltage source (VSI – Voltage Source Inverter) and is connected to batteries (master). The other inverters present act like current sources (slaves), following the reference from the VSI.

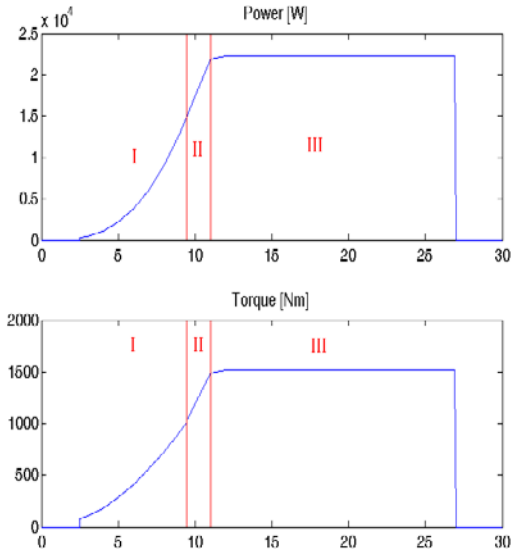

Fig. 4. Example of the separation in operating regions used to model wind turbines (horizontal axis: wind speed in m/s)

3.1 Voltage Source Inverter Model (VSI)

A central aspect of the modelling of the adequately the VSI is the control of the active and reactive powers, so the principles used to model this are now described.
The selfsync control approach, as proposed in Papathanassiou et al. (2004) and Engler (2004), is assumed to be used by the inverters to achieve parallel operation without the need for communication between them. The modelling of the selfsync control structure is schematized in Figure 5, with the following main components:

1. *Power acquisition* estimates the active and reactive powers from the measured current and voltage.
2. *Decoupling* filters the active and reactive powers using a first order system.
3. *Droops* implement a Droop algorithm to select the frequency, phase and amplitude for the *voltage reference* so that

$$U_{ref} = |u|\sin(2\pi ft + \varphi) \tag{18}$$

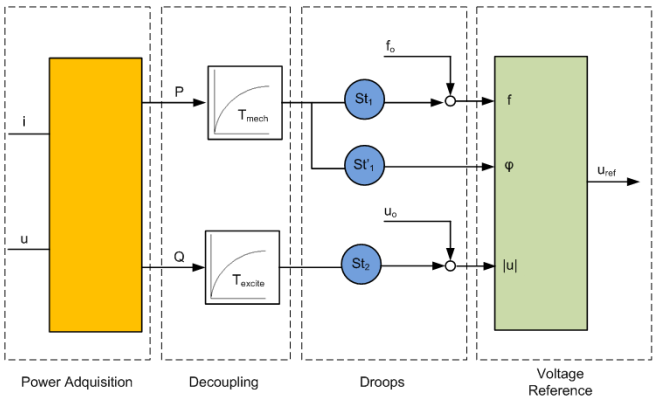

Fig. 5. Control approach simulated in the VSI

3.2 Current Source Inverters (CSI) Model

In this library, the microsources are given by PV arrays and a wind turbines, which are equipped with power electronic interfaces (DC/AC or AC/DC/AC) and a local controller to regulate production levels of active and reactive power. A current source configuration is assumed, so that they inject active power only into the grid.

Following a standard droops algorithm, the selected active power is proportional to the measured deviation of the MicroGrid frequency. Storage devices (batteries or supercapacitors) would inject or absorb active power to drive the frequency deviation to zero.

Correcting any permanent frequency deviation during islanded operation is the main objective for CSI control. In order to provide adequate secondary control to restore the frequency to the nominal value after any disturbance, a local secondary control is used, which is simulated in the library as a PI controller installed at each controllable MicroSource (except for solar inverters, where MPP control is used). This PI controller in the MicroSource computes the real power set point (P* in Figure 6) so that the frequency will return to the nominal value. This control action ensures that the MicroSources would produce the right amount of power (see Madureira et al. (2005) for details of the algorithm).

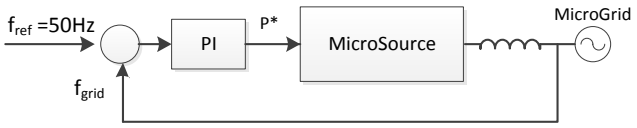

Fig. 6. Secondary load-frequency control at a MicroSource

4. VALIDATION

4.1 Component validation

Once the models were implemented as EcosimPro components, each of them was tested by comparing them with published or experimental results. For example, for a certain PV panel the I/V curve was evaluated at certain values (changing from 200W/m^2 to 1KW/m^2 in 200W/m^2 intervals): see Figure 3 for some results that fit adequately with results in the literature.

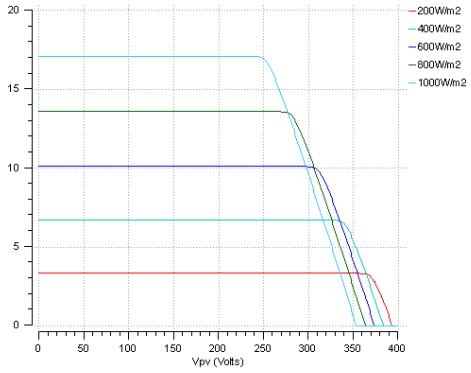

Fig. 7. Validation of PV array characteristics (I-V curve)

4.2 Microgrid simulation

Once the individual components were validated the connection of components was also tested. As an example, the results of the validation on a PV/Wind microgrid considering three-phase balanced operation are now discussed. Figure 8 shows the graphical implementation of this microgrid using components from the library. System parameters are as follow: A photovoltaic generator made up of 80 silicon mono-crystalline PV modules, each with a peak capacity of 185 Wp (giving a total of 14.8kW DC) and a wind turbine with peak power of 5 kW per line. A power profile analysis was done on the main components of the plant, which allowed the correct operation of the equipment to be checked.

As an example, the simulated effect of a load lower than designed, under quick changes in the energy sources is now presented: For the system in Fig. 8, sudden changes in the effective solar radiation are simulated, considering, for simplicity, a constant load of 1kW per phase and the turbine operating providing 1.2kW per phase.

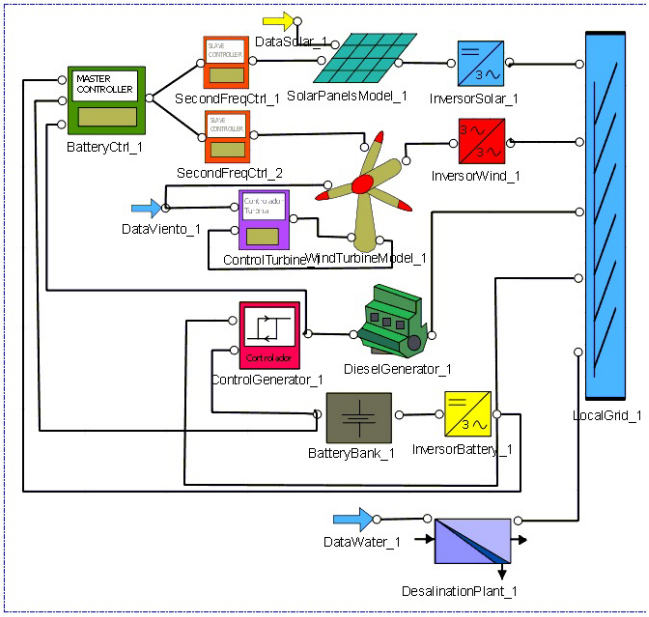

Fig. 8. Graphical implementation using the developed library of the case study (PV+Wind microgrid)

As expected, the power generated by the PV array is reduced by the frequency-based power control algorithm: the active power transmitted from the PV array (*PSolar* in Figure 9) is smaller than the possible peak power (*PMPPT*). To generate this frequency-based power control algorithm acts on the open circuit voltage reference (Vpvg) to obtain the desired power (see Figure 10, where the evolution of the selected Open Circuit Voltage reference is compared with the one that would provide the maximum power).

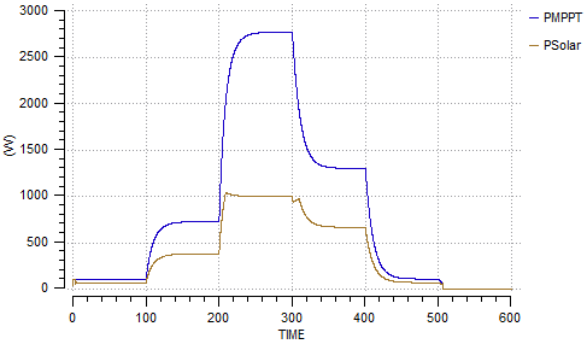

Fig. 9. Evolution of the Active Power generated by the PV Array in the validation experiments

In parallel, the output power ***PTurbine***, is also modified by the frequency-based power control algorithm in order to contribute to the reduction of power. In the configuration simulated the excess of energy (difference between the generated power and the power sent to the load) is dissipated in a resistor: alternative configurations based on temporary storage would be easily simulated using the provided library; deferrable loads could also be simulated using components from other EcosimPro libraries.

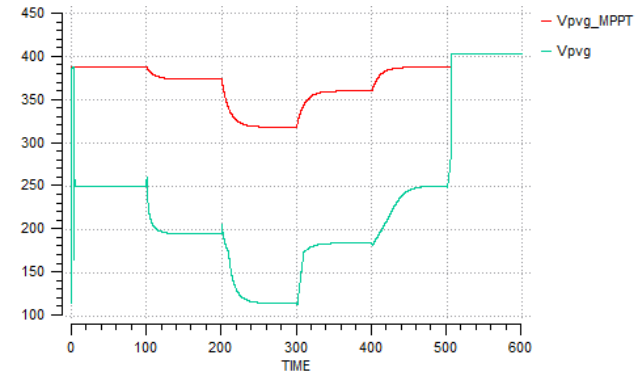

Fig. 10. Open Circuit Voltage reference Vpvg

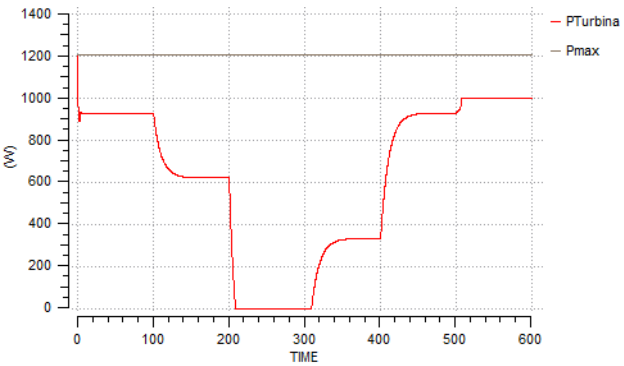

Fig. 11. Evolution of the Active Power generated by Wind Turbine in the validation experiments

To complete the presentation of the validation experiment presented, Figure 12 shows how the grid frequency is regulated: variations in the microgrid frequency makes possible to detect power imbalances; frequency returns to the nominal value of 50Hz once these disturbances are rejected.

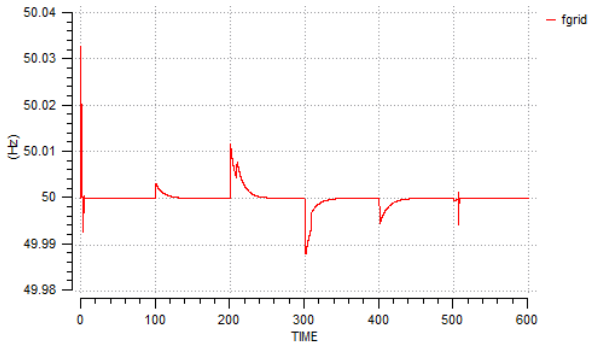

Fig. 12. Evolution of the Microgrid Frequency in the validation experiments

5. CONCLUSIONS

A preliminary library for the simulation of MicroGrids integrated by a variety of renewable MicroSources such as PV arrays and wind turbines has been presented, that was developed so that they can be integrated with existing models of loads, and the interactions reproduced, in order to simulate the operation during long periods of time. Further work is being done to develop additional components used in Microgrids (flywheels, supercapacitors, electrolyzers, fuel cells, etc), validate the simulations using a real Microgrid, and integrate the library with other EcosimPro libraries.

REFERENCES

Chouder, A., Silvertre, S., and Malek, A. (2006). Simulation of photovoltaic grid connected inverter in case of grid-failure. *Revue des Energies Renouvelables*, pp. 285 – 296.

Engler, A. (2004). Vorrichtung zum gleichberechtigten Parallelbetreb von einoder dreiphasigen Spannungsquellen. *European patent N° 02018526.26.*

Gambier, A., Wolf, M., Miksch, T., Wellenreuther, A., & Badreddin, E. (2009). Optimal systems engineering and control co-design for water and energy production: A European project. *Desalination and Water Treatment*, 10(1-3), 192-199.

Garcia, A., Acebes, L. F., & Prada, C. (2002). Modelling and simulation of batch processes: a case study. *Proc. 15th IFAC World Congress*, Barcelona.

Madureira, A., Moreira, C., and Lopes, J. A. P. (2005), Secondary load-frequency control for microgrids in islanded operation. *Proc. Int. Conf. Renewable Energy Power Quality*, Zaragoza, Spain.

Mei, F., and Bikash, C. (2005). Modelling and small-signal analysis of a grid connected doubly-fed induction generator. *Proc. IEEE PES General Meeting*, San Francisco, USA.

Mohammedi, K., Sadi, A., Belaidi, I., Bouziane, A., & Boudieb, D. (2011). Simulation and Exergy Analysis of a Small Scale Seawater Desalination/Electricity Production Prototype Powered with Renewable Energy. *Int. J. of Thermal & Environmental Engineering*, 2(2), 107-112.

Moral, J., Vara, R. P., Steelant, J., & De Rosa, M. (2010). ESPSS Simulation Platform. *Proc. 2010 Space Propulsion Conference,* San Sebastián, Spain, pp. 3-6.

Ordonez, L., Lasseur, C., Poughon, L., & Waters, G. (2004). MELiSSA higher plants compartment modeling using ecosimpro. *Society of Automotive Engineers,* Paper 01-2351.

Palacin, L. G., Tadeo, F., Elfil, H., de Prada, C., & Salazar, J. (2011). New dynamic library of reverse osmosis plants with fault simulation. *Desalination and Water Treatment*, *25*(1-3), 127-132.

Papathanassiou, S., Georgakis, D., Hatziargyriou, N., Engler, A., and Hardt, Ch. (2004). Operation of a prototype Micro-grid system based on MicroSource equipped with fast-acting power electronic interfaces. *Proc. 31th PESC,* Aachen, Germany.

Pérez-Vara, R., Mannu, S., Pin, O., & Müller, R. (2003). Overview of European Applications of EcosimPro to ECLSS, CELSS, and ATCS. *Proc. International Conference on Environmental Systems(ICES)*.

Raiambal, K., and Chellamuthu, C. (2002). Modelling and simulation of grid connected wind electric generating system. *Annals of IEEE TENCON,* pp. 1847-1852.

Rasila, M. (2003). Torque- and Speed Control of a Pitch Regulated Wind Turbine. *Thesis for the Master of Science Degree*, Chalmers University of Technology, Goteborg, Sweden.

Sallem, S., Chaabene, M., Kamoun, M.B.A. (2009). Optimum energy management of a photovoltaic water pumping system, *Energy Conversion and Management,* Volume 50, Issue 11, pp. 2728–31.

Salazar, J., Tadeo, F., and Prada, C. (2010a). Renewable Energy for Desalinization using Reverse Osmosis. *International Conference on Renewable Energies and Power Quality (ICREPQ'10),* Granada, Spain.

Salazar, J., Tadeo, F., de Prada, C., and Palacin, L. (2010b). Modelling and control of MicroGrid in Island Operation. *International Renewable Energy Congress,* Tunisia.

Salazar, J., Tadeo, F., Witheephanich, K., Hayes, M., and de Prada, C. (2011a). Control for a Variable Speed Wind Turbine equipped with a Permanent Magnet Synchronous Generator (PMSG). *Sustainability in Energy and Buildings (SEB'11),* Marseille, France.

Salazar, J., Tadeo, F., de Prada, C., and Palacin, L. (2011b). Modelling and Simulation of Auxiliary Energy Systems for off-grid Renewable Energy Installation. *International Renewable Energy Congress,* Hammamet, Tunisia.

Tara, Á.A., Martínez, E.H., & de Seoane, A.M.V.V. (2003), Modelling and Analysis with Ecosimpro of a Nuclear Power Plant Heat Sink Based on a Cooling Pond. *Proc. 2nd Meeting of EcosimPro Users*, Madrid, Spain.

Trishan, E., and Patrick, L. (2007). Comparison of Photovoltaic Array Maximum Power Point Tracking Techniques. *IEEE Transactions on Energy Conversion,* 22(2).